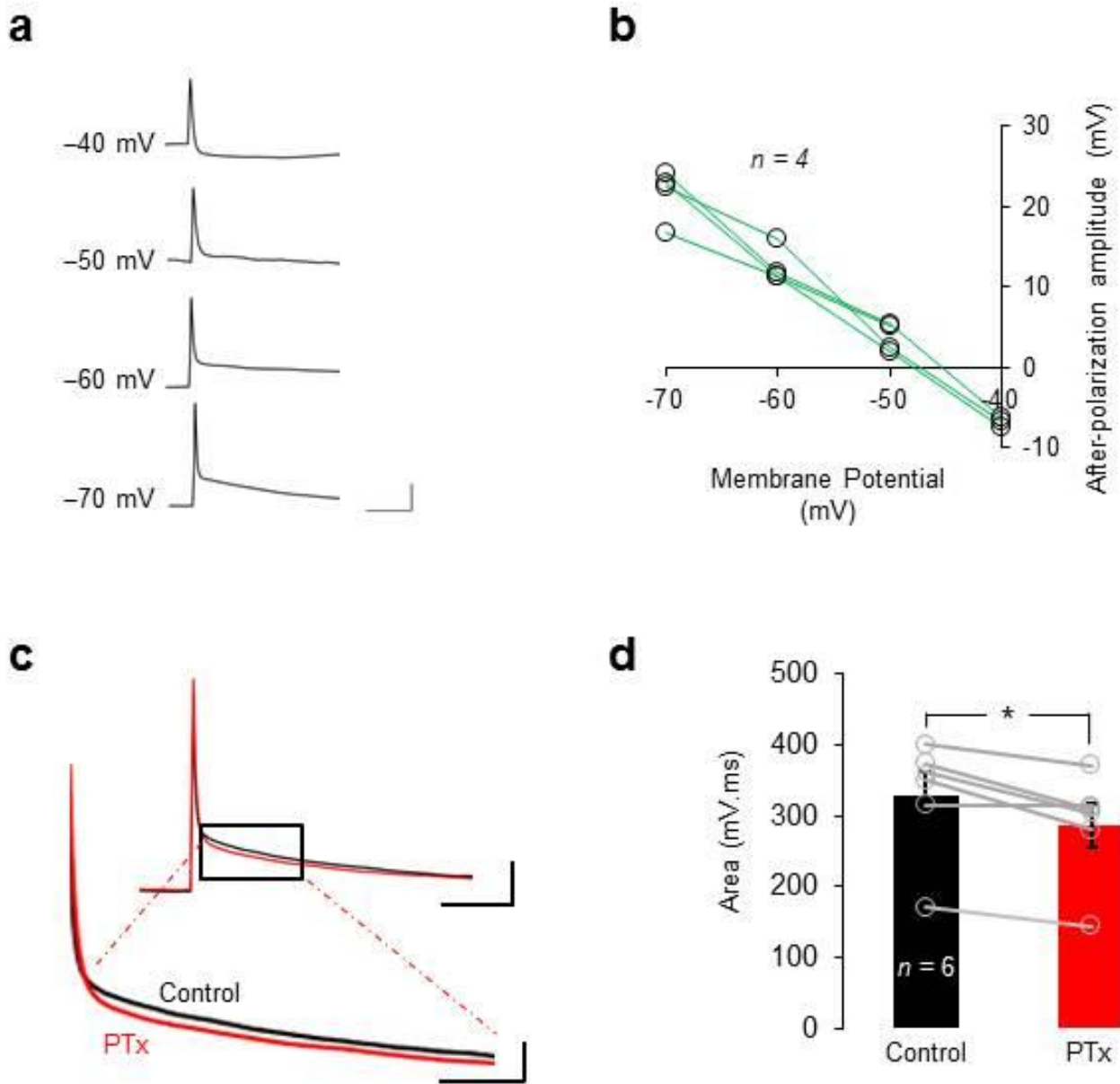


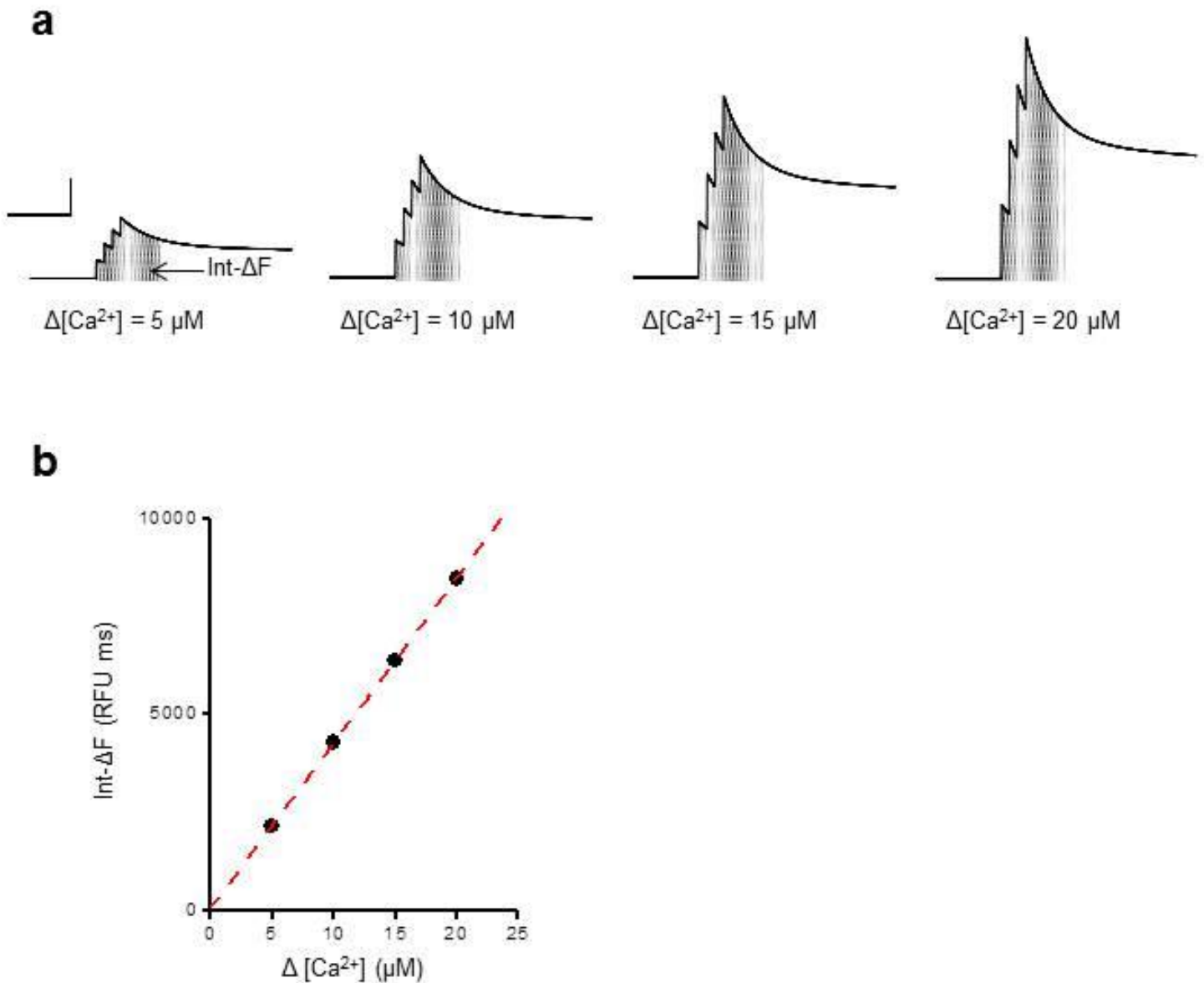
Supplementary Fig. 1: Properties of basket cell terminals.

(a) Prolonged depolarizing currents failed to elicit repetitive firing. Representative traces from one bouton in response to 500 ms depolarizing and hyperpolarizing 40 pA current pulses. Scale: 20 mV, 200 ms (main traces), 20 mV, 5 ms (insets). (b) Action potentials evoked by 55 Hz and 100 Hz trains of 1 ms depolarizing pulses, scale: 20 mV, 100 ms. (c) Action potential broadening at 55 Hz or 100 Hz in wild type and *Kcna1^{V408A/+}* mice.



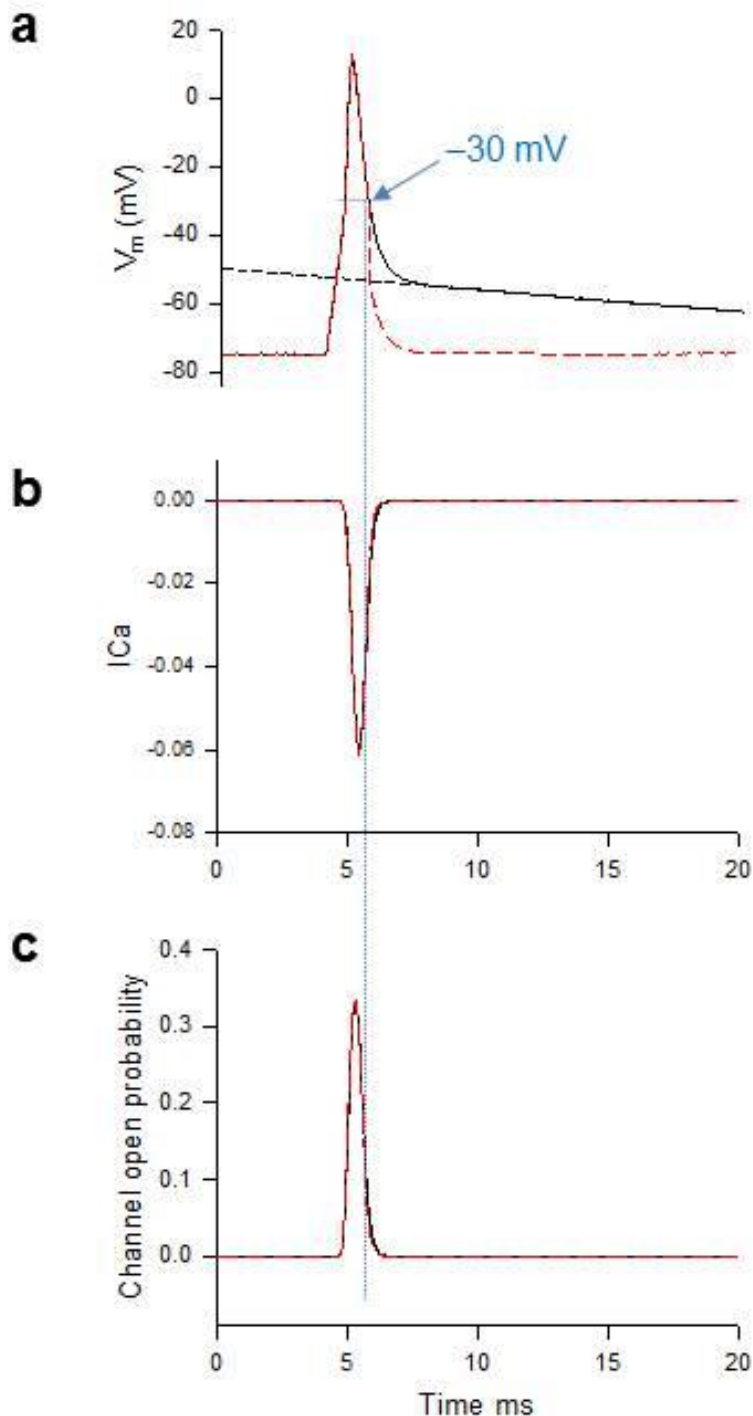
Supplementary Fig. 2. Bouton ADP properties.

(a) Representative traces from one bouton showing reversal of the ADP around -48 mV. Scale: 20 mV, 20 ms. (b) Summary data. (c) Representative traces from one bouton showing the effect of GABA_A receptor blockade with picROTOXIN (PTx). Scale: 20 mV, 20 ms (main traces); 5 mV, 5 ms (expanded trace). (d) PTx only decreased the ADP area measured over the initial 20 ms by a small amount (baseline: 329 ± 34 mV.ms; PTx: 287 ± 31 mV.ms). * $p < 0.05$, paired t test, $n = 6$.



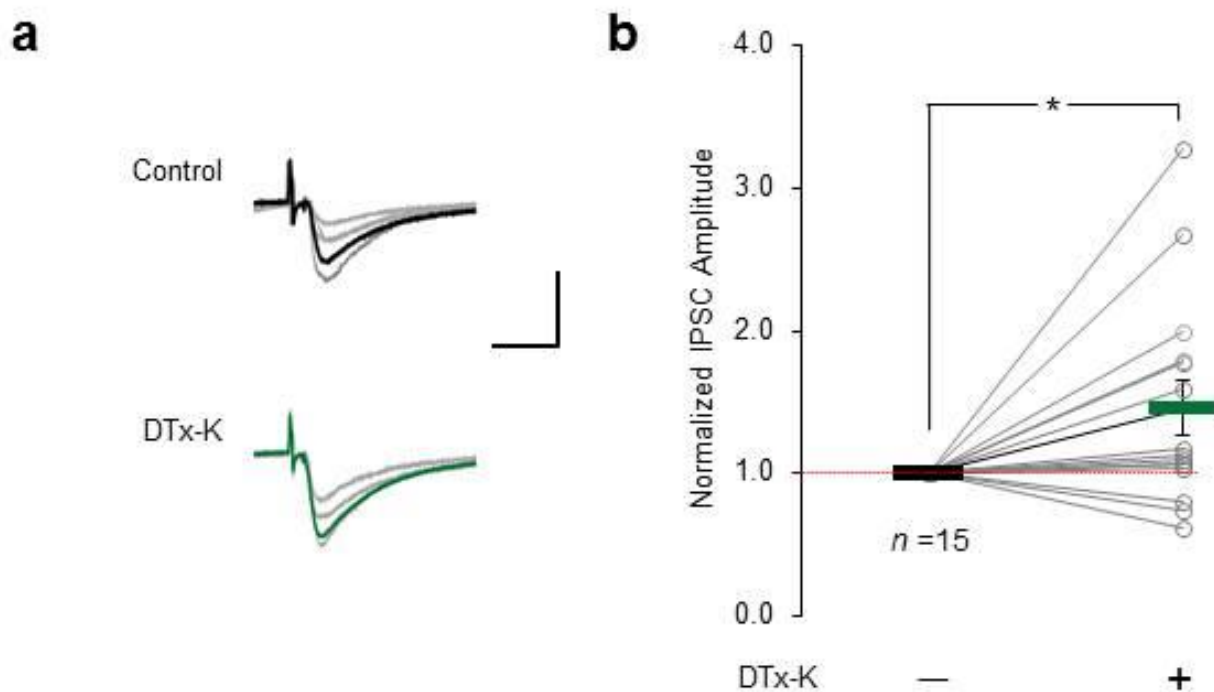
Supplementary Fig. 3. Fluo-4 fluorescence integrated over 200 ms (Int- ΔF) is proportional to total action potential-evoked $\Delta[\text{Ca}^{2+}]$.

(a) Fluo-4 Ca^{2+} fluorescence responses to a 40 Hz burst of 4 action potentials, simulated using a non-stationary single compartment model of presynaptic Ca^{2+} dynamics for different values of $\Delta[\text{Ca}^{2+}]$ per action potential. Shaded area under the traces corresponds to the integral of Fluo-4 fluorescence over 200 ms, starting with the beginning of stimulation (Int- ΔF). This was used as a measure of action potential-evoked $\Delta[\text{Ca}^{2+}]$. Scale: 10 RFU, 200 ms. (b) Linear relationship between Int- ΔF and $\Delta[\text{Ca}^{2+}]$.



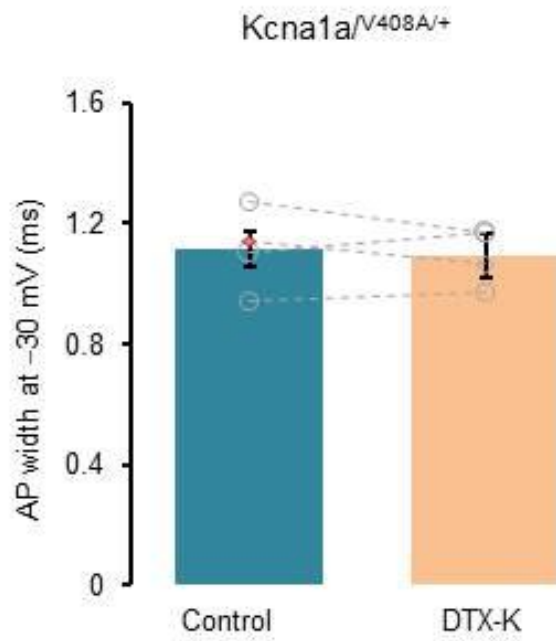
Supplementary Fig. 4. The ADP has a small effect on Ca^{2+} entry.

(a) The ADP was modelled by fitting a straight line to the slow voltage relaxation following a representative presynaptic action potential (dashed black line). It was then subtracted from the action potential waveform, starting when the membrane potential passed the -30 mV point (dashed red line). (b) Simulated Ca^{2+} current using six-state model (black: control; dashed red: without ADP). (c) Estimated open probability. Subtracting the ADP decreased the total integrated Ca^{2+} current by ~3%.



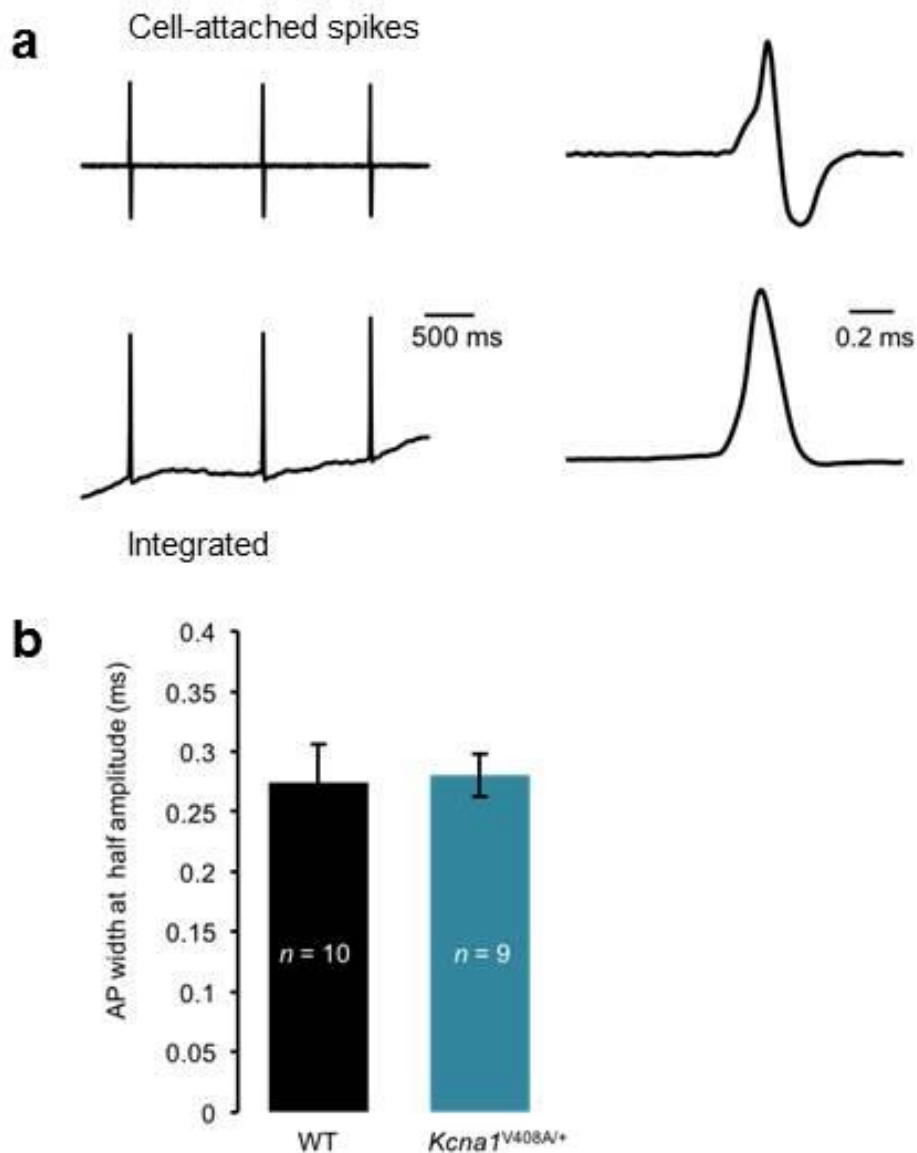
Supplementary Fig. 5. Effect of DTx-K on IPSCs recorded in wild type cerebellar Purkinje cells.

(a) Representative data from one experiment. Grey traces are individual sweeps; black and green traces are averages. Scale: 200 pA, 5 ms. (b) Summary of data. * $p < 0.05$, paired t test.



Supplementary Fig. 6. No effect of DTx-K on presynaptic spike width in *Kcna1*^{V408A/+} mice.

Summary of spike widths before and after DTx-K.



Supplementary Fig. 7. No difference in Purkinje cell spike width in *Kcna1*^{V408A/+} mice.

(a) Sample trace from one experiment showing cell-attached recording (top) and after numerical integration to estimate the spike width (bottom). Right: expanded time-base. (b) Comparison of wild type and *Kcna1*^{V408A/A} neurons. Between 15 and 61 spikes were measured in each Purkinje cell.

Supplementary Table 1: Passive membrane properties and action potential threshold.

	WT	<i>Kcna1</i>^{V408A/+}
RMP	-68.8 ± 1.5 mV (n = 9)	-68.6 ± 2.3 mV (n = 10)
Spike threshold	-43.2 ± 1.1 (n = 13)	-41.0 ± 0.9 (n = 21)
Rheobase	15.7 ± 1.2 pA (n = 7)	10.8 ± 4.7 pA (n = 6)
Input resistance	1.1 ± 0.2 G Ω (n = 8)	1.4 ± 0.2 G Ω (n = 9)
τ	11.8 ± 1.4 ms (n = 7)	12.2 ± 1.0 ms (n = 9)